

https://doi.org/10.1070/QEL17004

Temperature drift contribution to frequency instability of silicon Fabry–Perot cavities

N.O. Zhadnov, G.A. Vishnyakova, K.S. Kudeyarov,
D.S. Kryuchkov, K.Yu. Khabarova, N.N. Kolachevsky

Abstract. **A contribution of a temperature drift near the silicon thermal expansion coefficient zero point to the fractional frequency instability of a silicon cavity is analysed. The thermal expansion coefficient of silicon is measured by an optical method near the zero point T_0 = 123 K. It is shown that the frequency instability due to cavity temperature drifts observed in an experiment does not exceed a thermal noise limit at averaging intervals of up to 20 s.**

Keywords: *ultrastable cavities, single-crystal silicon, optical method for measuring thermal expansion coefficient, temperature drift, fractional frequency instability.*

1. Introduction

Progress in the development of ultrastable laser systems as precision measurement instruments stimulates many research fields. Without lasers having a sub-Hertz spectral linewidth, many modern experiments would be impossible, such as measuring the proton charge radius from the spectroscopic data on hydrogen atom [1], search for a drift of the fine structure constant [2], detection of a topological mass defect as one of the dark matter forms [3], gravitational wave detection [4, 5], etc. Note that modern optical frequency standards based on single ions or ensembles of ultracold atoms include ultrastable lasers. The frequency of such a laser is periodically (with the period of 1 s) adjusted to the frequency of a spectrally narrow well-studied 'clock' transition, which provides the frequency reference accuracy and long-term stability [6, 7]. The heart of an ultrastable laser system is a high-Q reference Fabry–Perot cavity, which is not sensitive to various exciting factors and, thus, provides a highly stable cavity length. The radiation frequency of such a laser stabilised by a transmission (or reflection) peak centre, for example, according to the Pound–Drever–Hall method [8], is also highly stable.

An ultrastable Fabry–Perot cavity is a pair of coaxial mirrors attached by optical contact to the cavity spacer, which fixes the distance between the mirrors and has an axial hole. Materials of the spacer and mirrors and their geometrical shape are chosen so that to reduce the influence of temperature variations and external vibrations and to minimise the thermal noise limit. The thermal noise of the spacer and mirrors of ultrastable cavities is thoroughly considered in [8], and so we will only write out the estimation formula, which demonstrates an influence of the main factors on the limiting instability of the cavity as a whole:

$$\sigma_y \sim \frac{T^{1/2}\varphi_{\mathrm{coat}}^{1/2}}{L^{5/4}\lambda^{1/2}E_{\mathrm{sub}}^{1/2}}, \tag{1}$$

where σ_y is the Allan deviation at the averaging time of 1 s; T is the cavity temperature; φ_{coat} is the loss angle (a reciprocal Q-factor) of the reflection coating material; L is the cavity length; λ is the radiation wavelength; and E_{sub} is Young's modulus of the cavity mirror substrate. This formula describes the contribution of the reflection coating thermal noise to frequency instability, which dominates in most cavity configurations.

Presently, the most common material for making ultrastable cavities is ULE glass produced by the flame hydrolysis deposition (it is sitall admixed with titanium oxide) or glass ceramics [9]. An important distinction of ULE glass is the zero thermal expansion point at room temperature, which in the case of a stabilised cavity temperature makes it possible to reduce substantially the sensitivity of mode frequency to slow temperature deviations. For a long time, systems with such cavities have demonstrated the best characteristics [10, 11]; however, since 2012 it was shown that silicon cavities may exhibit several orders higher stability, which is determined by thermal noise. First of all, this relates to a higher mechanical Q-factor of crystal silicon [12]. In addition, some drawbacks inherent in glass are absent in silicon cavities: there is no linear frequency drift caused by material ageing [13], which is due to the crystal structure and high thermal conductivity; the zero point has no shift [14], production technology of single-crystal silicon in Russia is more available than of ULE analogues.

Prospects for enhancing stability of the laser systems based on ULE cavities mainly imply increasing the cavity length according to formula (1) [11]. Evidently, there are

N.O. Zhadnov, G.A. Vishnyakova, K.S. Kudeyarov, D.S. Kryuchkov
P.N. Lebedev Physical Institute, Russian Academy of Sciences, Leninsky prosp. 53, 119991 Moscow, Russia;
K.Yu. Khabarova P.N. Lebedev Physical Institute, Russian Academy of Sciences, Leninsky prosp. 53, 119991 Moscow, Russia; Federal State Unitary Enterprise 'All-Russian Scientific-Research Institute of Physical-Technical and Radiotechnical Measurements', Mendeleevo, 141570 Moscow region, Russia; e-mail: kseniakhabarova@gmail.com;
N.N. Kolachevsky P.N. Lebedev Physical Institute, Russian Academy of Sciences, Leninsky prosp. 53, 119991 Moscow, Russia; Federal State Unitary Enterprise 'All-Russian Scientific-Research Institute of Physical-Technical and Radiotechnical Measurements', Mendeleevo, 141570 Moscow region, Russia; Russian Quantum Centre, ul. Novaya 100, Skolkovo, Moscow, 143025 Russia

Received 12 March 2019; revision received 27 March 2019
Kvantovaya Elektronika **49** (5) 424–428 (2019)
Translated by N.A. Raspopov

reasonable technical limitations and stronger requirements to temperature stabilisation and cavity suspension [15]. On this background, silicon cavities look more promising; the thermal expansion coefficient of silicon turns to zero at temperatures near 124 and 17 K and is very small in a temperature range of 0–4 K [16]. Low temperature also reduces the level of cavity thermal noise. Silicon systems are specific in that those can stabilise lasers only in the near-IR spectral range (1.2–15 μm), which is determined by a transparency window of the mirror silicon substrates through which radiation passes. In some applications, it is convenient because the spectral range of 1.5 μm is widely used in communication lines [17] and corresponds to the emission wavelength of erbium lasers including femtosecond systems [18].

In the leading world laboratories, ultrastable laser systems based on silicon cavities play the role of highly stable reference oscillators (similarly to the hydrogen standard in the RF range), which, with the help of a femtosecond frequency comb, additionally stabilises clock lasers in various wavelength ranges of atom and ion spectroscopy. For example, the employment of a laser additionally stabilised by a cryogenic silicon cavity in an optical clock on strontium atoms made it possible to reach a record value of fractional frequency instability (6×10^{-19}) at the averaging time of 1 hour [7].

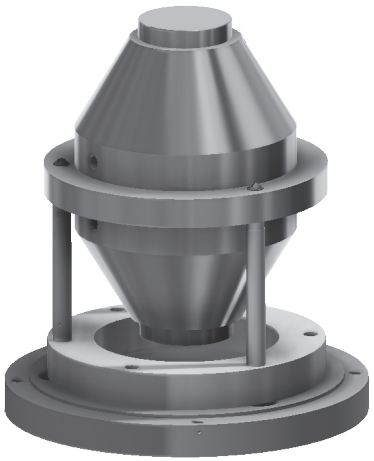

Figure 1. Silicon cavity of a biconical shape with a support in the centre-of-mass plane.

Attaining the level of thermal noise is a problem comprised of many subtasks, which can be divided into two groups: suppressing factors affecting the stability of cavity length and factors that hinder the exact referencing – feedback noise. The present work considers and investigates the contribution of a temperature drift near the zero point of silicon thermal expansion 124 K to the frequency instability of silicon cavities.

2. Influence of temperature variations on frequency instability

At the LPI laboratory, we have fabricated two identical systems for stabilising the frequency of NKT Photonics Koheras Adjustik lasers with the radiation wavelength $\lambda = 1.542$ μm by the transmission peak of cryogenic silicon cavities (Fig. 1) with dielectric mirrors. The identical systems give a chance to search for the zero point of thermal expansion and investigate the fractional frequency instability of the laser systems. The laser radiation frequency is stabilised to the TEM_{00} cavity mode by the Pound–Drever–Hall locking technique; the spectral width of the resonance peak is 3.5 kHz. The cavity length is $L = 78$ mm, which corresponds to the mode separation FSR = 1.92 GHz. High-frequency (up to 100 kHz) phase noise is suppressed by a high-frequency component of the servo signal, which controls the frequency of an acousto-optical modulator arranged directly after the laser, because fast modulation of the radiation frequency in the laser scheme is absent. Slow frequency deviations are compensated for by a low-frequency piezoelectric actuator, which varies the length of a fibre laser cavity. A simplified schematic of the experimental setup is shown in Fig. 2. Silicon cavities are placed in high-vacuum cryostats (Fig. 3) at a pressure of $\sim 10^{-9}$ mbar. The cavities are cooled due to radiative heat exchange with a nitrogen reservoir through two thermal shields (*2*) and (*3*) fabricated from anodised aluminium (Fig. 3), on which temperature sensors are arranged (thermistors PT100 in the four-contact circuit). A required temperature is stabilised by a heater arranged on shield *3*. The cryostat design realised in this way makes it possible to efficiently insulate the cavity from temperature fluctuations of the environment at a considerably low consumption of liquid nitrogen as compared to the flow scheme [12].

In order to find the frequency instability of the cavity mode related to a temperature drift, it is necessary to deter-

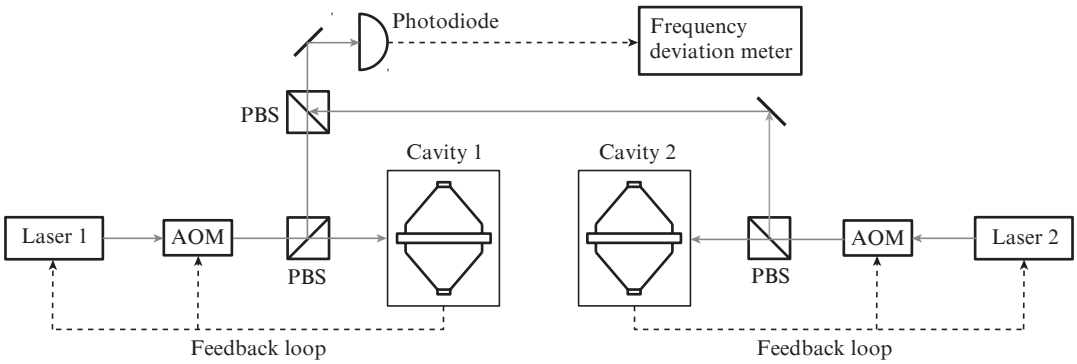

Figure 2. Simplified scheme for stabilisation and frequency measurement: (AOM) acousto-optic modulator; (PBS) polarisation beam splitter; (PD) photodiode.

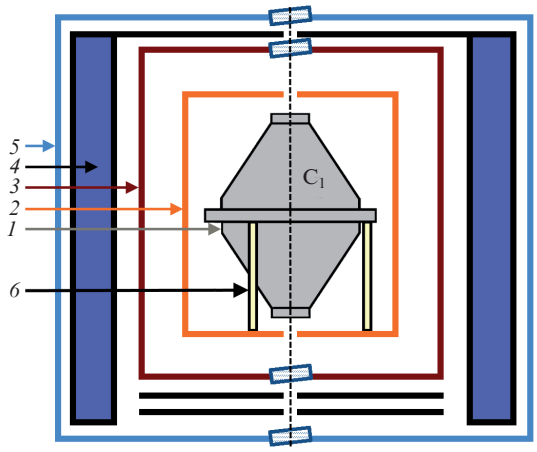

Figure 3. Schematic of the cryostat:
(*1*) cavity fabricated from single-crystal silicon; (*2*) passive thermal shield; (*3*) active thermal shield; (*4*) reservoir with liquid nitrogen; (*5*) external wall of cryostat; (*6*) cavity mounting made of PEEK; dashed line is the cavity optical axis.

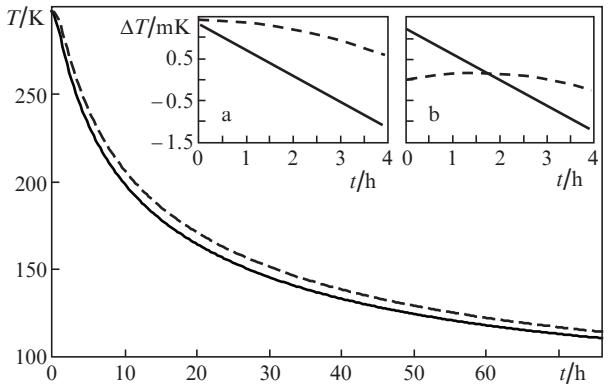

Figure 4. Cryostat cooling from room to liquid nitrogen temperature. The solid line is the measured temperature of heat shield *2* vs. time, the dashed line is the cavity spacer temperature recovered according to (2) vs. time. In the insets: temperature drift of shield *2* (solid curve) and calculated temperature drift of the cavity (dashed curve) in the regime of temperature stabilisation when the initial temperatures of shield *2* and cavity are equal (a) and when those differ by 1 mK (b).

mine the instability of cavity temperature and its influence on the frequency instability. To transfer from the temperature instability to the frequency instability, the thermal expansion coefficient of silicon is required, which can be found from the dependence of cavity mode frequency on temperature. Direct measurements of the cavity temperature cannot be realised in our system because a temperature sensor arranged on the cavity spacer would inevitably increase the cavity sensitivity to temperature and vibrations. Therefore, we recovered the evolution of cavity temperature by calculation methods issuing from the temperature of shield *2* and initial cavity temperature.

The heat exchange equation for shield *2* and the cavity is as follows:

$$C_1\dot{T}_1(t) = \beta[T_2^4(t) - T_1^4(t)] + \gamma[T_2(t) - T_1(t)]. \qquad (2)$$

Here, $C_1 = 132$ J K^{-1} is the heat capacity of silicon cavity; T_1 and T_2 are the temperatures of the cavity and thermal shield *2*, respectively; and the coefficient β is responsible for the intensity of radiative heat exchange, and γ refers to the heat exchange through supports on which the cavity is arranged, due to heat conduction. The value of β depends on albedo of the shield and cavity surfaces, their shapes and mutual disposition and is calculated according to [19]. The coefficient γ characterises the rate of heat transfer through three supports (Fig. 3) fabricated from a ceramic material (PEEK) with a low heat conductivity. In our case, $\beta = 7.29 \times 10^{-10}$ W K^{-4}, $\gamma = 2.60 \times 10^{-4}$ W K^{-1}. In the temperature range 100–300 K, the radiative contribution to the heat exchange is more than an order of magnitude that of heat conduction. According to (2), the dependence of cavity temperature on time was calculated by the temperature of shield *2* in the process of cryostat cooling from room to nitrogen temperature. At the initial instant, the temperatures of the cavity and nearest thermal shield were taken equal. The temperature evolution obtained is shown in Fig. 4. One can see that the temperature of cavity spacer follows that of shield *2* at a certain delay.

Of particular interest is the temperature range 120–126 K, which includes the zero point. The thermal expansion coefficient in this range was calculated from the measured frequency of beat signal f_{beat} between lasers stabilised by the modes of the cavities (*1*) and (*2*) in the cooling process described above (see Fig. 2). The temperature of cavity *2* maintained constant and was 123.5 K, which corresponds to the zero point value determined previously for this cavity. Data obtained and the following third-order polynomial interpolation are presented in Fig. 5, which illustrates that at certain temperature the beat frequency has the extremum. Then, the dependence of heat expansion coefficient on temperature is found (Fig. 6):

$$\alpha = \frac{\mathrm{d}\ln L}{\mathrm{d}T} = -\frac{\mathrm{d}\ln f_{\text{beat}}}{\mathrm{d}T}, \qquad (3)$$

and the zero point T_0 is calculated, which is approximately 123 K. Due to inaccuracy of model (2), the calculation error for this temperature may be large; therefore, we corrected

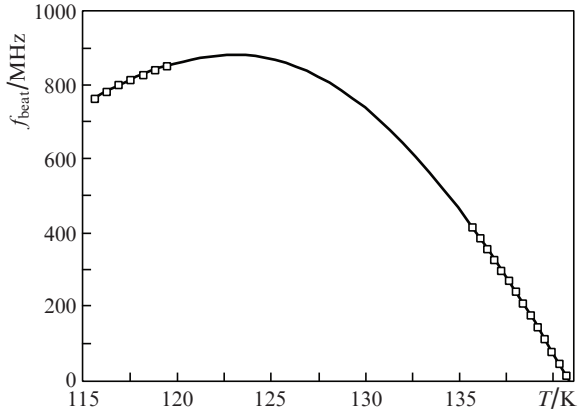

Figure 5. Dependence of emission beat frequency of lasers stabilised by the TEM_{00} mode of cavities 1 and 2 on temperature in the course of cooling one of the systems. Points refer to experimentally measured frequency, the solid line is Hermite interpolation.

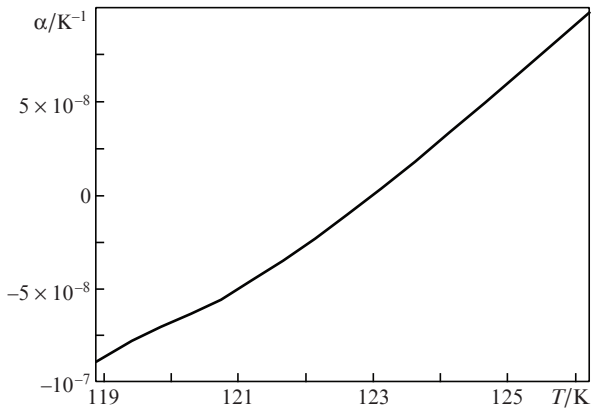

Figure 6. Temperature variation of the thermal expansion coefficient $\alpha(T)$ near the zero point of silicon, calculated from the dependence of beat frequency on time in the cooling process.

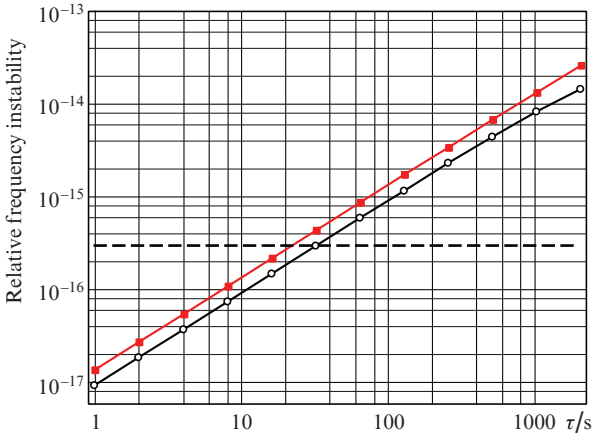

Figure 7. Calculated contribution of temperature fluctuations of the cavity spacer to the frequency instability. The cavity temperature is recovered from the measured shield temperature and recalculated to frequency deviations. The upper dependence corresponds to calculation with equal initial temperatures of shield and cavity (Fig. 4b) and is approximated by the linear drift function $\sigma_y(\tau) = 1.3 \times 10^{-15}\Delta T\tau$; the lower dependence is the case of the temperatures differing by 1 mK (Fig. 4a) [$\sigma_y(\tau) = 7.4 \times 10^{-16}\Delta T\tau$]. The temperature offset from the zero point is $\Delta T = 0.01$ K.

the zero point by the standard method from [10]. Nevertheless, the frequency measurements performed give important information about TEM_{00} mode position at the zero point and can be used for more accurate temperature adjustment.

A separate task is studying temperature drifts in the regime of temperature stabilisation. We have performed long-term measurements of the temperature drift at shield *2*, which was about 0.7 mK h^{-1}. The drift may be related to variations of room temperature, which affect the temperature of the external shield of cryostat (shield *5* in Fig. 3) and lead to drifts in control electronics. From data obtained, we calculated the cavity temperature evolution for two different cases: when the initial temperatures of the cavity and external shield are equal (Fig. 4a), and when those differ by ~1 mK (Fig. 4b). Assuming that the error of zero point determining due to inaccuracy of temperature setting ΔT is 10 mK and taking the thermal expansion coefficient at this point $\alpha(T_0 \pm \Delta T) \approx 2.8 \times 10^{-10}$ K^{-1}, one can calculate the temperature instability from the instability of cavity frequency.

The corresponding Allan deviation $\sigma_y(\tau)$ is shown in Fig. 7. The thermal noise level calculated for our silicon cavities is 3×10^{-16} [15]. At times up to 20 s, the fractional frequency instability due to temperature drift does not exceed the thermal noise level; it is important for employing such systems in frequency standards. However, one should take into account that the instability estimates obtained above depend on the temperature offset from the zero point. For example, at a temperature offset of 100 mK, the contribution to the frequency instability will be approximately equal to that of thermal noise at the averaging time of 2 s. Generally, for reducing system sensitivity to variations of ambient temperature, an additional thermal insulation and thermo-stabilisation of certain electronic units is desirable.

3. Conclusions

Temperature drifts of a reference cavity are important limitations of the final frequency instability in laser systems locked to cavity modes. For the system considered, analysis of the fractional frequency instability of silicon cavity mode shows that the contribution of temperature instability does not exceed that of thermal noises at an averaging time of less than 20 s and accuracy of zero-point stabilisation of 10 mK. This fully complies with most of precision spectroscopy tasks and applications in the field of optical frequency standards. For employing developed silicon cavities as high-stability reference oscillators with the goal frequency instability at the level of 10^{-15} at long averaging time, it is necessary to either use additional thermal shield or transfer to helium temperatures.

An optical method is suggested for measuring a thermal expansion coefficient $\alpha(T)$, which makes it possible to determine the cavity zero point dynamically and is a valuable addition to the conventional method for determining the zero point of thermal expansion.

Acknowledgements. The work was supported by the Russian Foundation for Basic Research (Grant No. 16-29-11723).

References

1. Beyer A., Maisenbacher L., Matveev A., et al. *Science*, **358**, 79 (2017).
2. Rosenband T., Hume D.B., Schmidt P.O., et al. *Science*, **319** (5871), 1808 (2008).
3. Geraci A.A., Bradley C., Gao D., et al. arXiv:1808.00540v2 [astro-ph.IM] (2018).
4. Kwee P., Bogan C., Danzmann K., et al. *Opt. Express*, **20** (10), 459 (2012).
5. Kolkowitz S., Pikovski I., Langellier N., et al. *Phys. Rev. D*, **94** (12), 1 (2016).
6. Brewer S.M., Chen J.-S., Hankin A.M., et al. arXiv:1902.07694 [physics.atom-ph] (2019).
7. Oelker E., Hutson R.B., Kennedy C.J., et al. arXiv:1902.02741 [physics.atom-ph] (2019).
8. Kessler T., Legero T., Sterr U. *J. Opt. Soc. Am. B*, **29** (1), 178 (2012).
9. Gubin M.A., Kireev A.N., Konyashchenko A.V., et al. *Quantum Electron.*, **38** (7), 613 (2008) [*Kvantovaya Elektron.*, **38** (7), 613 (2008)].

10. Alnis J., Matveev A., Kolachevsky N., et al. *Phys. Rev. A*, **77** (5), 1 (2008).
11. Häfner S., Falke S., Grebing C., et al. *Opt. Lett*., **40** (9), 2112 (2015).
12. Kessler T., Hagemann C., Grebing C., et al. *Nat. Photon*., **6** (10), 687 (2012).
13. Hagemann C., Grebing C., Lisdat C., et al. *Opt. Lett*., **39** (17), 5102 (2014).
14. Legero T., Kessler T., Sterr U. *J. Opt. Soc. Am. B*, **27** (5), 914 (2010).
15. Zhadnov N.O., Kudeyarov K.S., Kryuchkov D.S., et al. *Quantum Electron*., **48** (5), 425 (2018) [*Kvantovaya Elektron*., **48** (5), 425 (2008)].
16. Robinson J.M., Oelker E., Milner W.R., et al. *Optica*, **6** (2), 240 (2019).
17. Droste S., Ozimek F., Udem T., et al. *Phys. Rev. Lett*., **111** (11), 110801 (2013).
18. Ohmae N., Kuse N., Fermann M.E., Katori H. *Appl. Phys. Express*, **10** (6), 062503 (2017).
19. Parma V. arXiv:1501.07154 [physics.acc-ph] (2015).